



Influence of Rubber Crumb Particle Size on Abrasive Behavior of Rubber Crumb Modified Epoxy Composites

Vishwas Mahesh^{a,*} 

^aDepartment of Industrial and Engineering Management, Siddaganga Institute of Technology, Tumakuru, Visvesvaraya Technological University, Belagavi, Karnataka, India.

Keywords:

Abrasion
Statistical optimization
Rubber crumb
Polymer composite
Analysis of variance

ABSTRACT

The study investigates the relationship between rubber crumb particle size and the abrasive behavior of polymer composites, using statistical optimization techniques. Polymer composites with different rubber crumb sizes were synthesized and subjected to abrasion tests. Taguchi's L18 orthogonal array was employed to analyze the effects of filler particle size (2 levels), filler weight percentage, load, and time (3 levels each) on the specific wear rate of the developed composites. Analysis of variance (ANOVA) revealed that particle size significantly influenced abrasion resistance, with a P-value of 0.073 and an F-value of 3.8 from Taguchi's Design of Experiments (DOE). Smaller particles exhibited milder abrasion, characterized by smoother surface interactions and lower material removal, while larger particles caused more aggressive abrasion due to rougher surfaces, larger contact areas, and higher stress concentrations. The findings highlight the pivotal role of rubber crumb particle size in tailoring the abrasive properties of polymer composites. This study provides a framework for optimizing material performance, offering significant potential for applications in sectors requiring durable and wear-resistant composites, such as automotive, construction, and aerospace.

* Corresponding author:

Vishwas Mahesh
E-mail: vishwasmahesh@gmail.com

Received: 12 November 2024

Revised: 2 January 2025

Accepted: 1 February 2025



© 2025 Published by Faculty of Engineering

1. INTRODUCTION

The increasing focus on sustainability and resource efficiency has led to significant interest in the use of recycled materials in polymer composites. Among these materials, rubber particles derived from waste tires have emerged as promising fillers due to their ability to improve mechanical and tribological properties while promoting

environmental sustainability. Rubber particles offer advantages such as elasticity, energy absorption, and damping properties, making them suitable for applications in the automotive, construction, and aerospace sectors. Despite these benefits, challenges remain in understanding the precise role of rubber particle characteristics, such as particle size, in influencing composite performance under abrasive conditions [1].

Polymer composites, owing to their versatility and tailorable properties, have gained considerable attention across diverse industrial sectors, ranging from automotive to construction [2,3]. Among various reinforcing agents used in polymer composites, rubber crumb particles have emerged as a promising additive due to their abundance, low cost, and potential to enhance mechanical properties [4,5]. These rubber crumb-reinforced polymer composites exhibit notable advantages such as improved impact resistance, damping properties, and sustainability [6]. However, a critical aspect influencing their performance, particularly in applications involving wear and abrasion, is the abrasive behaviour of these materials.

Polymer composites, fortified with fillers, have become instrumental in addressing the challenges of wear and friction in various tribological applications. Tribology, the study of friction, wear, and lubrication, encompasses a wide array of industries ranging from automotive and aerospace to manufacturing and biomedical fields [7]. In these applications, the demand for materials exhibiting superior tribological properties, such as enhanced wear resistance and reduced friction coefficients, is paramount [8]. Fillers play a crucial role in augmenting the tribological performance of polymer composites by modifying their surface morphology, interfacial interactions, and mechanical properties [9]. These fillers can be categorized into various types, including particulate fillers (e.g., nanoparticles, microspheres), fibrous fillers (e.g., carbon fibers, glass fibers), and lamellar fillers (e.g., graphite, molybdenum disulfide). Each type of filler offers distinct advantages and mechanisms for improving tribological properties [10].

Particulate fillers, particularly nanoparticles, exhibit a high surface area-to-volume ratio, leading to enhanced reinforcement and lubrication properties. Nanofillers such as nanoclays, carbon nanotubes, and graphene offer exceptional strength and lubrication at the nanoscale, thereby reducing friction and wear in tribological systems. The incorporation of fillers into polymer matrices for tribological applications involves careful consideration of factors such as filler dispersion, orientation, and compatibility with the polymer matrix. Achieving optimal dispersion and interfacial adhesion

between fillers and the polymer matrix is crucial for maximizing the tribological performance of composite materials [11,12].

Abrasion resistance is a crucial requirement for polymer composites utilized in applications subjected to wear, such as automotive components, conveyor belts, and industrial machinery parts [13,14]. The ability of a material to withstand abrasion and maintain its integrity directly impacts its service life and operational efficiency. Rubber crumb particle size is recognized as a key parameter influencing the abrasive behavior of polymer composites. The size distribution of rubber particles affects the interfacial adhesion between the rubber phase and the polymer matrix, as well as the overall microstructure of the composite material [15-18].

Existing research has predominantly focused on the mechanical properties of polymer composites reinforced with rubber particles, including their tensile and impact behavior. However, the abrasive behavior, which is critical for wear-intensive applications, has received limited attention. The relationship between rubber crumb particle size and specific wear resistance is particularly underexplored, creating a knowledge gap in optimizing the tribological properties of such composites. Moreover, while some studies have addressed the effects of particle size in general terms, there is a lack of systematic investigation into how different particle sizes interact with other factors, such as filler weight percentage, applied load, and abrasion time, to influence wear performance [1,19].

This study aims to address this gap by investigating the impact of rubber crumb particle size on the abrasive behavior of polymer composites using statistical optimization techniques. By employing Taguchi's L18 orthogonal array and analysis of variance (ANOVA), this research provides a quantitative framework to evaluate the interplay between particle size and other parameters affecting specific wear rate. The findings aim to establish a deeper understanding of the role of particle size in controlling abrasion resistance, providing practical insights for designing polymer composites with tailored properties [20-22].

The significance of this research extends beyond merely expanding the understanding of rubber particle-reinforced composites; it plays a pivotal role in the broader context of sustainable material innovation. By effectively integrating rubber waste into polymer matrices, this study not only enhances the mechanical and functional properties of composites but also addresses critical environmental concerns associated with waste management.

The global accumulation of discarded rubber, particularly from end-of-life tires, presents a significant challenge due to its slow degradation and harmful ecological impact. Through strategic incorporation of rubber particles in polymeric systems, this research demonstrates a viable pathway for repurposing rubber waste, reducing landfill accumulation, and lowering dependence on virgin materials.

Furthermore, optimizing the dispersion and interaction of rubber particles within the polymer matrix contributes to improving key material characteristics such as impact resistance, toughness, and damping properties, making these composites suitable for a wide range of industrial applications, including automotive, aerospace, and infrastructure. By aligning with the principles of circular economy and resource efficiency, this work not only supports sustainable manufacturing practices but also reinforces the role of advanced composite materials in achieving a greener and more resilient future.

2. MATERIALS AND METHODS

2.1 Materials

The suggested composites are made with epoxy L12 along with K6 hardener as matrix and waste rubber crumb as fillers. Epoxy matrix was obtained from CS Marketing, Bengaluru, Karnataka, India and Rubber crumb particles from Quality rubber components, Bengaluru, Karnataka, India. The properties of rubber crumb and epoxy used in the present study is provided in Table 1.

Table 1. Properties of rubber crumb.

Properties	Rubber Crumb	Epoxy
Density	0.95g/cm ³	1.1-1.4
Ultimate Tensile Strength	9 MPa	60-80
Elongation at break	150%	2.5-5%
Hardness (Shore A)	64	

2.2 Fabrication

The recommended composites were produced by the moulding process. Before filling the mould, the hardener K6 and epoxy L12 were properly combined in a 1:10 ratio using a stirrer. Wax coating was applied to the mould to facilitate laminate removal. After filling the mould, the mixture of resin and hardening agent was left to cure for a full day [23]. To create the suggested composites, the fillers was extensively combined and strengthened inside the resin system. The recommended composites' parameters are listed in Table 2.

Table 2. Composites and their designations.

Filler Size in μ	Filler content in wt%	Composite designation
212	20	C1
212	40	C2
212	60	C3
850	20	C4
850	40	C5
850	60	C6

2.3 Three body wear

According to ASTM G 65, three-body abrasive wear tests are conducted. The 75 mm x 25 mm x 3 mm created abrasive samples are cleaned before being installed on the specimen holder, and their initial weight is calculated using a high precision digital balance. The abrasive material is angular-shaped, sharp-edged AFS 60 silica sand. Figure 1 shows the testing arrangement, sand used and its SEM micrograph.

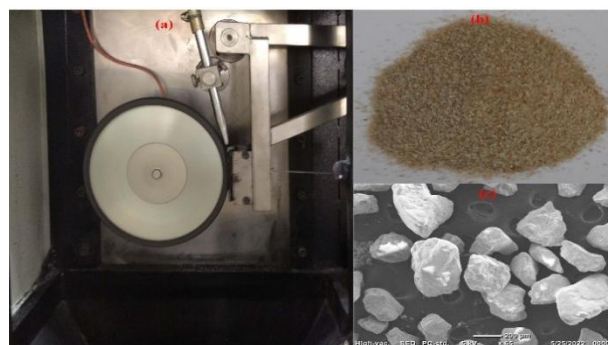


Fig. 1. (a) Testing arrangement; (b) Abrasive sand and (c) SEM micrograph of sand used.

The application requirements and the characteristics of the material being tested are taken into consideration while choosing the test parameters, such as the load (10, 20 and 30 N) and test period (10, 20 and 30 min). The test specimens

are mounted into the appropriate holders, and the apparatus is then set up to track the test parameters. The test is begun by giving the test specimens the chosen load and speed (200 rpm) and letting them run for the allotted amount of time. Abrasive flow was maintained at 200 ± 0.05 g/min.

The specimen's weight loss upon abrasion is determined using Eq. 1.

$$M_l = M_i - M_f \tag{1}$$

Where, M_l , M_i , M_f in g, represents loss in the mass of syntactic foam, initial mass of syntactic foam, and final mass of syntactic foam respectively.

Important process factors that might affect the abrasion rate or specific wear rate of a material are filler %, load, and time. These factors need to be carefully regulated, and their effects need to be carefully examined and understood in order to establish the ideal circumstances for minimizing wear. Taguchi's L18 orthogonal array was chosen for statistical optimization, obviating the need for additional, costly trials.

Table 3 lists the particular factors and levels that were employed in the current investigation to carry out the DOE L18 study.

Table 3. Particular factors and levels that were employed in the current investigation to carry out the DOE L16 study.

Factors	Level-1	Level-2	Level-3
Filler Particle size in μ : A	212 (L1)	850 (L2)	---
Filler weight percentage: B	20 (L1)	40 (L2)	60(L3)
Load (N): C	10 (L1)	20 (L2)	30 (L3)
Time (min): D	10 (L1)	20 (L2)	30 (L3)

Table 4 lists the various testing parameters used to produce the L18 orthogonal array.

Table. 4 Factors and testing conditions used in L18 orthogonal array.

A	B	C	D
212	20	10	10
212	20	20	20
212	20	30	30
212	40	10	10
212	40	20	20
212	40	30	30
212	60	10	20
212	60	20	30

212	60	30	10
850	20	10	30
850	20	20	10
850	20	30	20
850	40	10	20
850	40	20	30
850	40	30	10
850	60	10	30
850	60	20	10
850	60	30	20

Recommended composites' density is found by using Archimedes' water displacement principle. To get the specific rate of wear in m^3/Nm , Eq. 2 is used.

$$K_s = \frac{V_l}{LD} \tag{2}$$

where D is the sliding distance (m), L is the applied load (N), and V_l is the volume loss (m^3). The composite's volume loss is computed using Eq. 3.

$$V_l = \frac{M_l}{\rho} \tag{3}$$

where density in g/m^3 is represented by ' ρ '. To transform angular motion into linear velocity, use the formula 4, while Equation 5 is used to calculate sliding distance.

$$V = 0.10472Nr \tag{4}$$

where V (m/s), r (m), and N (RPM) represent the linear velocity, radius of rubber disc and angular velocity of the rubber disc used in the rig, respectively.

$$D = VT \tag{5}$$

Where time in seconds is represented by 'T'. Further, the damaged area is studied under a microscope to identify the abrasion mechanism.

3. RESULTS AND DISCUSSION

3.1 S/N ratio

L18 orthogonal design developed by Taguchi is used for the trials. The mass loss along with the specific wear rate are displayed in Table 5. S/N ratio for "smaller is better" is determined using Eq.6. S/N ratios are found for lowest weight loss with the "smaller is better" criteria since it is preferred that the composite lose less weight

$$S/N = -10 \log_{10} \left(\frac{(\Sigma y^2)}{n} \right) \tag{6}$$

The letters 'n' and 'y' stand for the overall number of responses and the number of responses for the chosen factor level combination, respectively.

Both, the response of the composite and its particular wear rate, along with the influence of the factors on the wear rate, were assessed. Table 5 provides a summary of the responses for Signal-to-noise ratios.

Table 5. Sp. rate of wear of proposed composites under various test circumstances.

A	B	C	D	Loss of mass (g)	Sp. rate of wear x 10 ⁻⁵ (m ³ /Nm)
212	20	10	10	4	1.67
212	20	20	20	3	4.17
212	20	30	30	3	1.85
212	40	10	10	2	1.67
212	40	20	20	2	4.17
212	40	30	30	2	1.85
212	60	10	20	2	8.33
212	60	20	30	2	2.78
212	60	30	10	3	5.56
850	20	10	30	3	5.56
850	20	20	10	4	8.33
850	20	30	20	2	2.78
850	40	10	20	2	8.33
850	40	20	30	3	2.78
850	40	30	10	3	5.56
850	60	10	30	2	5.56
850	60	20	10	2	8.33
850	60	30	20	1	2.78

Table 6 demonstrates that filler particle size (A) having rank 1 has greatest influence on effect on sp. wear rate. Figure 2 displays the optimum level of each factor affecting wear rate.

Table 6. ANOVA indicating the percentage contribution of various factors

Factor	Degrees of freedom	F value	P Value
Filler particle size in μ	3	3.8	0.073
Filler wt%	3	1.42	0.254
Load	3	2.04	0.177
Time	3	2.04	0.177
Error	3		
Total	15		
S= 0.175281, R-sq = 91.91 %, R-sq (adj) = 90.78%			



Fig. 2. Signal to noise ratio of various factors and their levels.

The filler particle size with 212 μ, a weight percentage of 20 wt% with load and time at 30N and 30 minutes respectively are preferred (A1B1C3D3).

3.2 ANOVA

Analysis of Variance (ANOVA) is a powerful statistical method used to assess whether there are significant differences between the means of two or more groups or treatments. It achieves this by decomposing the total variability in the dataset into distinct components corresponding to different sources of variation. The primary goal of ANOVA is to evaluate whether the observed variations in the data can be attributed to actual differences among the groups or if they are merely due to random chance. The fundamental principle behind ANOVA is to compare the within-group variance (variation within each treatment or group) and the between-group variance (variation among different treatment groups). If the between-group variance is significantly larger than the within-group variance, it suggests that at least one group mean is different from the others, leading to the rejection of the null hypothesis, which assumes no difference between the groups. In this study, ANOVA has been employed to analyze weight loss data, helping to determine whether the differences in weight loss across various conditions or material compositions are statistically significant. Table 6 presents the detailed ANOVA results, including key statistical indicators such as the sum of squares (SS), degrees of freedom (df), mean square (MS), F-value, and p-value. The F-value is particularly crucial as it indicates the ratio of the between-group variance to the within-group variance, while the p-value helps

in assessing whether the differences are statistically significant. A p-value below a predetermined significance level (e.g., 0.05) would indicate that the variations in weight loss are not due to random chance but are instead influenced by the factors under investigation. By providing insights into the statistical significance of the results, the ANOVA analysis presented in Table 6 aids in making informed conclusions about the impact of different treatments or material formulations on weight loss, thereby supporting the overall findings of the study.

The factor rows represents the variation in the dependent variable that is due to differences between the "Filler particle size", "Filler wt %", "Load" and "Time". The F-ratio for filler particle size is 3.8. Finally, the p-value for the same is 0.073, which is less amongst the all, indicating that filler particle size has a significant effect on the dependent variable. ANOVA table indicates that the filler particle size has a significant effect on the dependent variable, as evidenced by the large F-ratio and small p-value for the filler particle size.

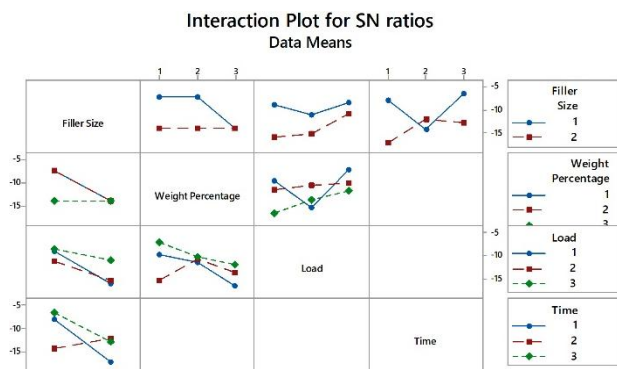


Fig. 3. Interaction plot for specific rate of wear.

Figure 3 shows the interaction plot for SN (Signal-to-Noise) ratios shows how various factors, including Filler Size, Weight Percentage, Load, and Time, influence the output (e.g., specific wear rate). Filler Size and Weight Percentage exhibit a potential interaction effect, as the lines are not parallel, indicating that their joint influence varies on the SN ratios. A weak interaction is seen between Filler Size and Load, with slight divergence of the lines, while a moderate interaction is observed between Filler Size and Time, as the lines show some divergence. Weight Percentage and Load show a significant interaction, with non-parallel lines

indicating that the effect of weight percentage varies greatly with load. A moderate interaction is noted between Weight Percentage and Time, with the lines being fairly non-parallel. The strongest interaction occurs between Load and Time, with non-parallel lines suggesting their combined effect on the SN ratios depends on test duration. Key observations indicate that optimizing the specific wear rate requires considering the combined influence of these factors, as most interactions show non-parallel lines, with significant interactions between Weight Percentage and Load, and Load and Time.

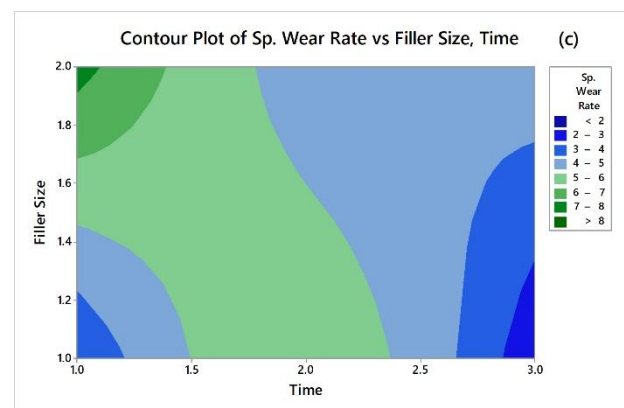
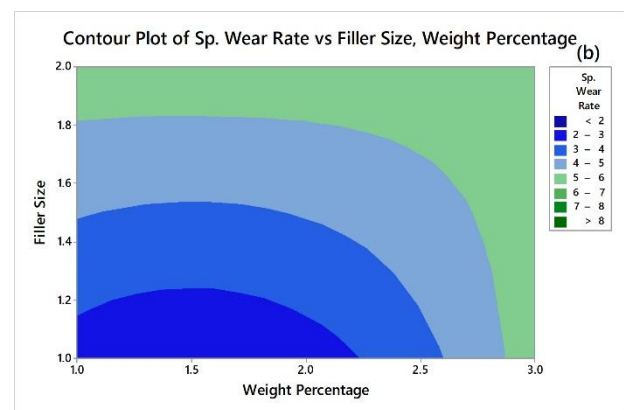


Fig. 4. Contour plot of (a) specific wear rate vs filler size, load; (b) specific wear rate vs filler size, weight percentage and (c) specific wear rate vs filler size, time.

Figure 4 shows the contour plot of specific wear rate indicating influence of both fillers. It is evident that the minimum specific wear rate region is obtained when filler size in minimum and load is maximum; filler size is minimum and weight percentage is minimum and filler size is minimum and time maximum.

3.3 Analysis of wear morphology

In worn out composite samples exposed to abrasion, three distinct zones-entry (Zone 1), middle (Zone 2), and exit (Zone 3) may be seen from Figure 5. Zones 1 and 2, where the silica sand exerted the least pressure, had surface damage that was consistent with particle rolling. These results show that initially, the wear rates on fresh surfaces are rather high, but they eventually start to fall as the abrading distance rises. This is because imperfections and inhomogeneity are quickly eliminated until a smooth, uniform surface is created.

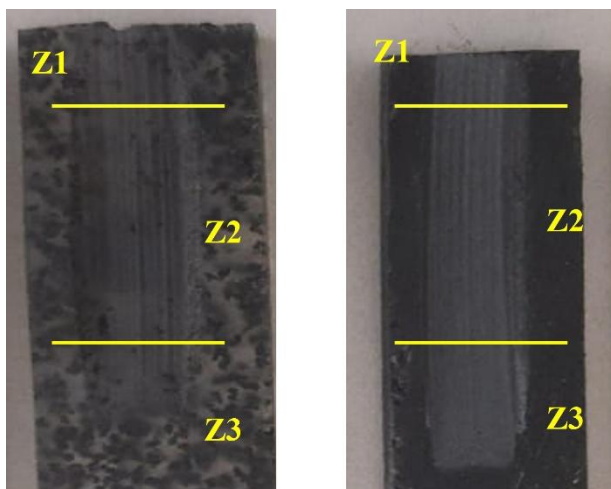
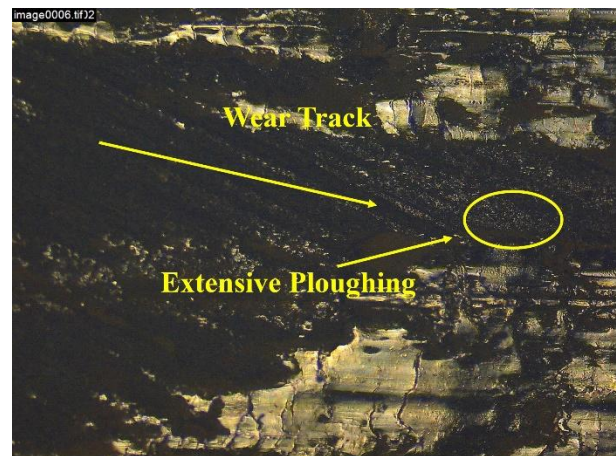


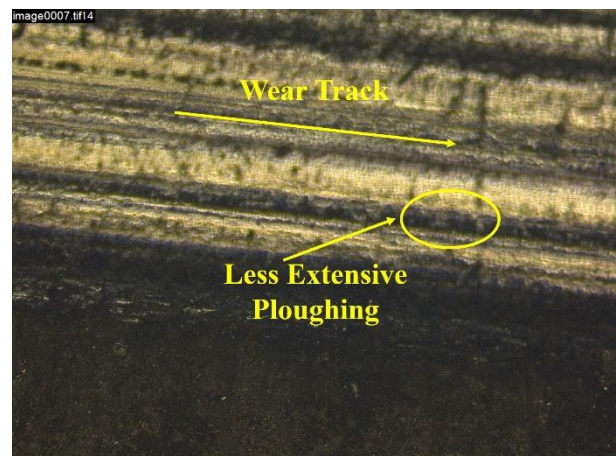
Fig. 5. Different zones of wear on the composites.

Figure 6 shows the mechanism of wear in developed composites. Smaller rubber crumb particles typically have smoother surfaces compared to larger particles. While they still have some irregularities, these are less pronounced than those found on larger particles. Smaller particles have a smaller contact area with the counter-surface during sliding. As a result, the localized pressures at the contact interface are lower compared to larger particles. Due to their smaller size, 212-micron rubber crumb particles penetrate less deeply into the polymer matrix during sliding. This results in less extensive plowing and cutting of the matrix material. The

contact stresses are more evenly distributed over the smaller contact area, reducing the likelihood of significant stress concentrations and localized material removal. Abrasive wear in composites reinforced with 212-micron rubber crumb particles is primarily characterized by mild abrasion, where the smoother surfaces of the particles glide over the counter-surface with relatively lower levels of material removal.



C5



C2

Fig. 6. Mechanism of wear in developed composites (a) C5 Configuration and (b) C2 configuration.

Figure 6 shows the mechanism of wear in developed composites. Smaller rubber crumb particles typically have smoother surfaces compared to larger particles. While they still have some irregularities, these are less pronounced than those found on larger particles. Smaller particles have a smaller contact area with the counter-surface during sliding. As a result, the localized pressures at the contact interface are lower compared to larger particles. Due to their smaller size, 212-

micron rubber crumb particles penetrate less deeply into the polymer matrix during sliding. This results in less extensive plowing and cutting of the matrix material. The contact stresses are more evenly distributed over the smaller contact area, reducing the likelihood of significant stress concentrations and localized material removal. Abrasive wear in composites reinforced with 212-micron rubber crumb particles is primarily characterized by mild abrasion, where the smoother surfaces of the particles glide over the counter-surface with relatively lower levels of material removal.

Larger rubber crumb particles have rougher surfaces with more pronounced irregularities compared to smaller particles. These irregularities enhance abrasive action during sliding. Larger particles have a larger contact area with the counter-surface, leading to higher localized pressures at the contact interface. Due to their larger size, 850-micron rubber crumb particles penetrate more deeply into the polymer matrix during sliding. This results in more extensive plowing and cutting of the matrix material. The contact stresses are more concentrated over the larger contact area, leading to significant stress concentrations and localized material removal. Abrasive wear in composites reinforced with 850-micron rubber crumb particles is characterized by more aggressive abrasion, where the rough surfaces of the particles dig into the counter-surface, causing higher levels of material removal.

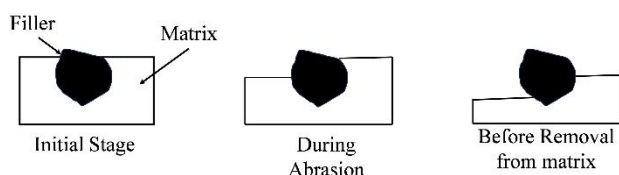


Fig. 7. Schematic of filler location during different stages of abrasion.

Figure 7 shows the schematic of filler location during different stages of abrasion. The amount of particle that protrudes over the working surface will continuously rise during the operation. Its retention strength in the composite will therefore decline owing to a reduction in the area of "adhesion," and the adhesive strength will also decline. In this instance, the force acting on the particle will intensify until it is finally eliminated from the composite's overall volume.

Figure 8 shows the composite surface with sand with rubber crumb oarticles following wear in the soil mass and clearly shows the locations where abrasive soil particles have scratched or cut the covering.

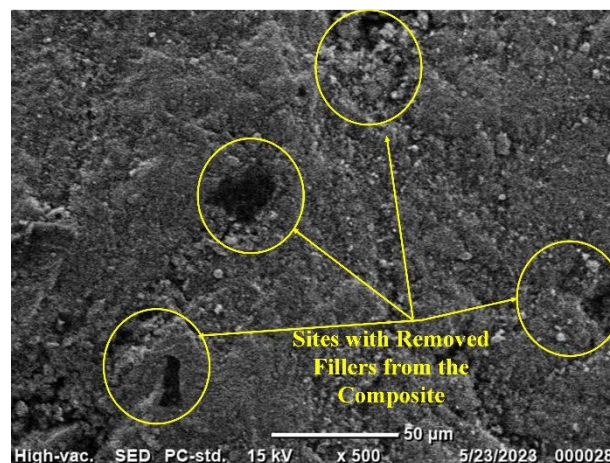


Fig. 8. SEM images showing formation of fox holes.

Figure 8 shows the composite surface with sand with rubber crumb oarticles following wear in the soil mass and clearly shows the locations where abrasive soil particles have scratched or cut the covering.

This confirms the results that were obtained. The slotted grooves are interrupted and then resurface, and they are positioned at a certain angle to the contact plane rather than being evenly dispersed throughout the surface. The passage of the wear medium over the surface at a certain angle is responsible for the groove arrangement ("foxholes") with relation to the horizontal. The interaction of soil particles with the composite surface causes the cutting zone to be interrupted because it comes into touch with the filler fractions and modifies their displacement vector.

4. CONCLUSION

The present study investigated the influence of rubber crumb particle size on the abrasive behavior of polymer composites using a statistical optimization approach. Through systematic experimentation and analysis, we elucidated key insights into how variations in particle size affect abrasive wear mechanisms in these composites. Our findings revealed significant differences in abrasive behavior between composites reinforced

with 212-micron and 850-micron rubber crumb particles. Smaller particles exhibited milder abrasion, characterized by smoother surface interactions and lower levels of material removal. In contrast, larger particles induced more aggressive abrasion due to their rougher surfaces, larger contact areas, deeper penetration depths, and higher stress concentrations. Moreover, our statistical optimization approach allowed us to identify optimal combinations of rubber crumb particle size and other factors to minimize abrasive wear in polymer composites.

The statistical optimization approach provided key insights into the optimal combinations of rubber crumb particle size and other contributing factors, allowing for the minimization of abrasive wear in polymer composites. This approach enables manufacturers to tailor composite formulations for enhanced wear resistance, thereby improving the longevity and performance of materials in diverse industrial applications.

By leveraging this approach, manufacturers and designers can tailor composite formulations to meet specific wear resistance requirements for various applications. The innovation of this study lies in the application of statistical method for optimizing the abrasive wear properties of polymer composites reinforced with rubber crumb particles, offering a systematic and quantifiable method to enhance material performance. However, some limitations, such as the variability of wear conditions in real-world applications and the need for more extensive testing across a broader range of particle sizes, should be addressed in future studies. The prospects of this research include expanding the analysis to include additional fillers and exploring the wear mechanisms in more complex environments. Ultimately, this study contributes valuable knowledge to the field of polymer composite development, providing a foundation for more durable and wear-resistant materials in various engineering sectors.

Declarations

Funding: This work was funded by Science and Engineering Research Board (SERB), Government of India through Teachers Association for Research Excellence (TARE) scheme TAR/2021/000016.

Competing Interest: The authors declare no competing interests.

Author Contribution: Vishwas Mahesh-Conceptualization, Investigation, Methodology, Project administration, Writing original manuscript, Formal analysis.

Acknowledgements: The author Vishwas Mahesh, acknowledged the support provided by Govt. of India through the SERB- TARE (TAR/2021/000016) project.

Data Availability: Data sharing does not apply to this article as no new data was created or analyzed in this study.

REFERENCES

- [1] A. P. Mouritz, E. Gellert, P. Burchill, and K. Challis, "Review of advanced composite structures for naval ships and submarines," *Compos. Struct.*, vol. 53, no. 1, pp. 21–42, 2001, doi: [10.1016/S0263-8223\(00\)00175-6](https://doi.org/10.1016/S0263-8223(00)00175-6).
- [2] S. H. Kamarudin, L. C. Abdullah, M. M. Aung, C. T. Ratnam, and E. R. Jusoh Talib, "A study of mechanical and morphological properties of PLA based biocomposites prepared with EJO vegetable oil based plasticiser and kenaf fibres," *Mater. Res. Express*, vol. 5, no. 8, 2018, doi: [10.1088/2053-1591/aabb89](https://doi.org/10.1088/2053-1591/aabb89).
- [3] B. Jena, B. Nayak, and S. Satapathy, "Physical & mechanical characterization of composites from waste tire rubber crumb," *Mater. Today Proc.*, vol. 26, no. 2, pp. 1752–1756, 2020, doi: [10.1016/j.matpr.2020.02.368](https://doi.org/10.1016/j.matpr.2020.02.368).
- [4] A. Thakur, K. Senthil, R. Sharma, and A. Singh, "Employment of crumb rubber tyre in concrete masonry bricks," *Mater. Today Proc.*, vol. 32, no. 4, pp. 553–559, 2020, doi: [10.1016/j.matpr.2020.02.106](https://doi.org/10.1016/j.matpr.2020.02.106).
- [5] A. Ali Emadi and A. Modarres, "Impact of crumb rubber particles on the fracture parameters of concrete through WFM, SEM and BEM," *Constr. Build. Mater.*, vol. 305, no. April, p. 124693, 2021, doi: [10.1016/j.conbuildmat.2021.124693](https://doi.org/10.1016/j.conbuildmat.2021.124693).
- [6] K. Agarwal, "Short Fibre and Particulate-reinforced Rubber Composites," *Def. Sci. J.*, vol. 52, no. 3, pp. 337–346, 2002, doi: [10.14429/dsj.52.2189](https://doi.org/10.14429/dsj.52.2189).
- [7] U. Nirmal, J. Hashim, and M. M. H. Megat Ahmad, "A review on tribological performance of natural fibre polymeric composites," *Tribol. Int.*, vol. 83, pp. 77–104, 2015, doi: [10.1016/j.triboint.2014.11.003](https://doi.org/10.1016/j.triboint.2014.11.003).

- [8] K. Friedrich, "Polymer composites for tribological applications," *Adv. Ind. Eng. Polym. Res.*, vol. 1, no. 1, pp. 3–39, 2018, doi: [10.1016/j.aiepr.2018.05.001](https://doi.org/10.1016/j.aiepr.2018.05.001).
- [9] H. Ismail, M. R. Edyham, and B. Wirjosentono, "Bamboo fibre filled natural rubber composites: the effects of filler loading and bonding agent," *Polym. Test.*, vol. 21, no. 2, pp. 139–144, 2002, doi: [10.1016/S0142-9418\(01\)00060-5](https://doi.org/10.1016/S0142-9418(01)00060-5).
- [10] W. Österle, A. I. Dmitriev, B. Wetzels, G. Zhang, I. Häusler, and B. C. Jim, "The role of carbon fibers and silica nanoparticles on friction and wear reduction of an advanced polymer matrix composite," *Mater. Des.*, vol. 93, pp. 474–484, 2016, doi: [10.1016/j.matdes.2015.12.175](https://doi.org/10.1016/j.matdes.2015.12.175).
- [11] P. Harsh Kumar, H. Chetan Kumar, S. Nitin, K. Pankaj V, and P. Subrata Kumar, "Effect of nano glass cenosphere filler on hybrid composite eigenfrequency responses - An FEM approach and experimental verification," *Adv. Nano Res.*, vol. 7, no. 6, pp. 419–429, 2019, doi: [10.12989/anr.2019.7.6.419](https://doi.org/10.12989/anr.2019.7.6.419).
- [12] B. Suresha, T. Jayaraju, P. R. S. Rao, M. Ismail, and K. N. Shivakumar, "Three-Body Abrasive Wear Behaviour of Fiber Reinforced Vinyl Ester Composites," *Solid State Phenom.*, vol. 136, pp. 99–108, 2008, doi: [10.4028/www.scientific.net/SSP.136.99](https://doi.org/10.4028/www.scientific.net/SSP.136.99).
- [13] B. N. Ramesh, B. Suresha, G. Chandramohan, and D. Anjaiah, "Three-body abrasive wear behaviour of microfiller-filled carbon-epoxy composites: A factorial design approach," *Compos. Interfaces*, vol. 18, no. 9, pp. 783–800, 2011, doi: [10.1163/156855412X629619](https://doi.org/10.1163/156855412X629619).
- [14] S. Kumar, B. Kuriachen, N. Kumar, and R. Nateriya, "The slurry abrasive wear behaviour and microstructural analysis of A2024- SiC-ZrSiO₄ metal matrix composite," *Ceram. Int.*, vol. 44, no. 6, pp. 6426–6432, 2018, doi: [10.1016/j.ceramint.2018.01.037](https://doi.org/10.1016/j.ceramint.2018.01.037).
- [15] B. Zhao, Y. Zhang, Y. Fan, X. Yu, Z. Zhang, and B. Zhang, "The three-body abrasive tribological characteristics of the Graphene/h-BN heterostructure film considering defects," *Tribol. Int.*, vol. 171, p. 107525, 2022, doi: [10.1016/j.triboint.2022.107525](https://doi.org/10.1016/j.triboint.2022.107525).
- [16] V. Mahesh, "Study on Slurry Erosion Resistance and Damage Mechanism in Cenosphere Reinforced Syntactic Foams for Light Weight Applications," *Int. J. Light. Mater. Manuf.*, 2023, doi: [10.1016/j.ijlmm.2023.11.004](https://doi.org/10.1016/j.ijlmm.2023.11.004).
- [17] V. Mahesh, "Comparative study on three body abrasive wear behaviour of natural compliant thermoplastic composite under dry and lubricated conditions," *J. Thermoplast. Compos. Mater.*, vol. 0, no. 0, pp. 1–17, 2023, doi: [10.1177/08927057231173592](https://doi.org/10.1177/08927057231173592).
- [18] V. Mahesh, V. Mahesh, S. M. Nagaraj, P. Subhashaya, and G. S. T. Shambu Singh, "Physio-mechanical and thermal characterization of jute/rubber crumb hybrid composites and selection of optimal configuration using the MADM approach," *Proc. Inst. Mech. Eng. Part C J. Mech. Eng. Sci.*, vol. 236, no. 14, pp. 7942–7952, 2022, doi: [10.1177/09544062221079166](https://doi.org/10.1177/09544062221079166).
- [19] V. Mahesh and V. Mahesh, "Tribological characterization of sustainable Jute-Epoxy-Rubber crumb hybrid composite," *Proc. Inst. Mech. Eng. Part C J. Mech. Eng. Sci.*, vol. 236, no. 19, pp. 10281–10289, 2022, doi: [10.1177/09544062221103941](https://doi.org/10.1177/09544062221103941).
- [20] S. R. K, "Taguchi and Regression analysis of abrasive wear behavior of carbon epoxy composite," *Journal of Materials and Engineering*, vol. 1, no. 2, pp. 68–73, Jan. 2023, doi: [10.61552/jme.2023.02.003](https://doi.org/10.61552/jme.2023.02.003).
- [21] P. R. Pati and M. P. Satpathy, "Investigation on red brick dust filled epoxy composites using ant lion optimization approach," *Polym. Compos.*, vol. 40, no. 10, pp. 3877–3885, 2019, doi: [10.1002/pc.25246](https://doi.org/10.1002/pc.25246).
- [22] A. H. P. S. Khalil *et al.*, "Incorporation of coconut shell based nanoparticles in kenaf/coconut fibres reinforced vinyl ester composites," *Mater. Res. Express*, vol. 4, no. 3, 2017, doi: [10.1088/2053-1591/aa62ec](https://doi.org/10.1088/2053-1591/aa62ec).
- [23] Atul Ltd. Polymer Division, "Technical Data Sheet Lapox L-12 K-6," 2020. [Online]. Available: <https://5.imimg.com/data5/VR/WS/MY-34403803/lapox-epoxy-resin-l12-with-hardener-k-6-1-1-kg-packing.pdf>.